SOLAR CELLS BASED ON SEMICONDUCTOR QUANTUM DOTS

Enrique A. Dalchiele

Instituto de Física, Facultad de Ingeniería, Montevideo, URUGUAY.

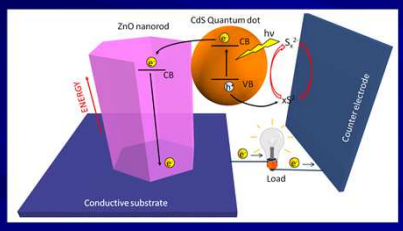

Introduction

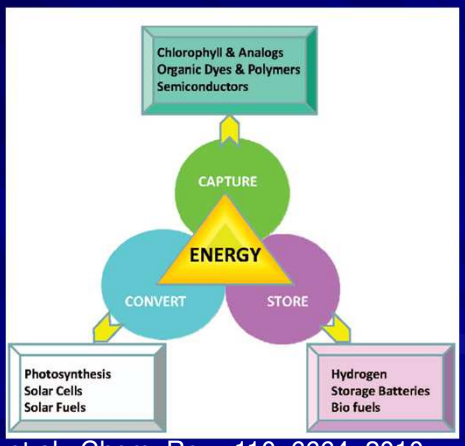

P.V. Kamat et al., Chem. Rev., 110, 6664, 2010.-

Solar cell concepts

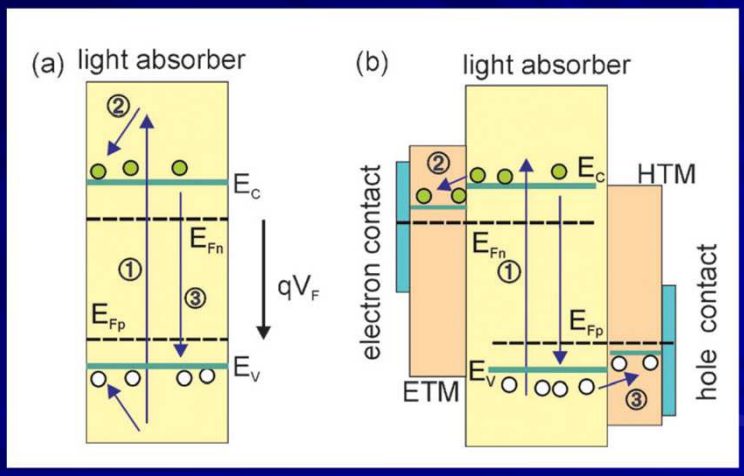

F. Fabregat-Santiago et al.,Phys. Chem. Chem. Phys.,13, 9083, 2011.-

Solar cell concepts

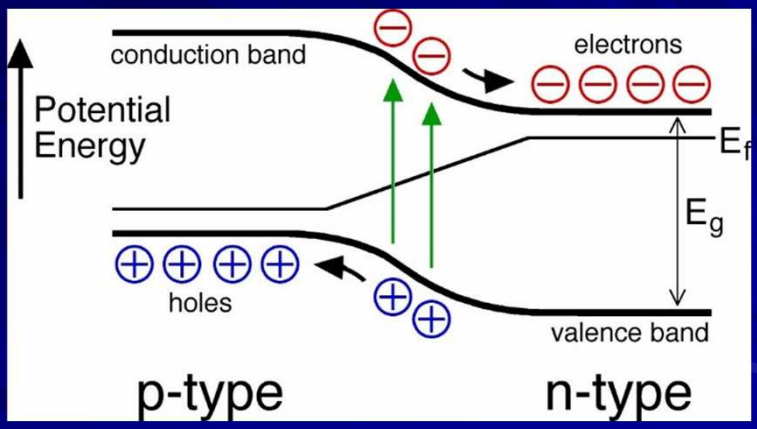

Solar cell concepts

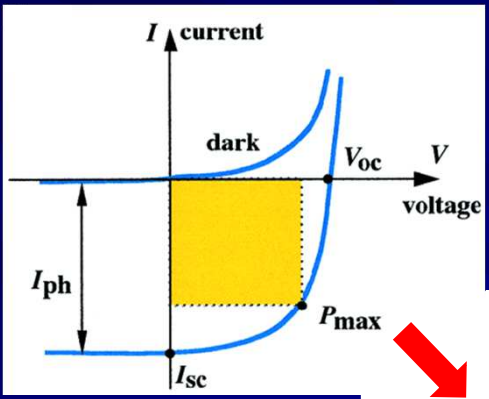

Energy-conversion efficiency, η.

$$\eta = \frac{V_{mp} J_{mp}}{P_{in}} = \frac{V_{oc} J_{sc} FF}{P_{in}}$$

Third generation solar cells

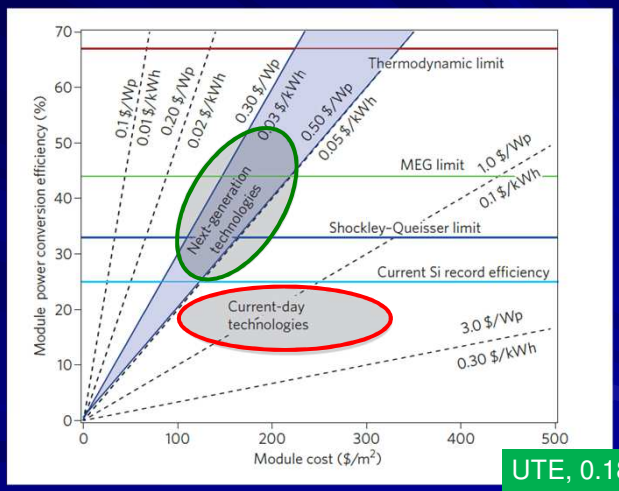

UTE, 0.18 U$S/kWh

What are Quantum Dots?

- Quantum dots are semiconductor nanocrystals that are so small they are considered dimensionless.
- Quantum dots range from 2-10 nm (10-50 atoms) in diameter.

Nanocrystal Quantum Dots

- Since m_h/m_e ~ 6 in CdSe, the electron levels are separated more widely than the hole levels.
- Wave functions corresponding to different *n* and/or *l* are orthogonal.
- Only optical transitions between states of the same symmetry can be observed.

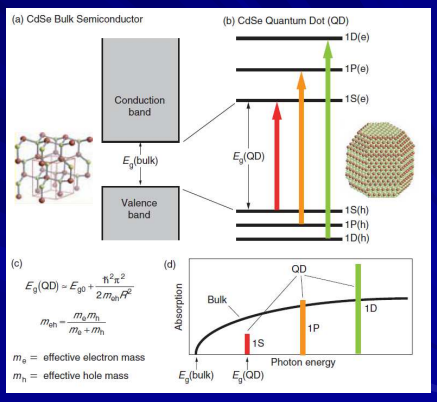

Exciton Bohr radius

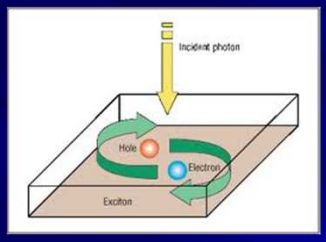

$$a_o = \frac{4\pi\varepsilon_o h^2}{m_e e^2}$$

$$a^* = \frac{\varepsilon}{m^*/m_e} a_o$$

a_o=0.53 Å
m effective electron mass*

Exciton Bohr radius and the bandgap energy

- Bandgaps, and therefore the energy associated with them, depend on the relationship between the size of the crystal and the exciton Bohr radius.
- Weak confinement regime, $R>>a_B$
- Strong confinement limit, $R<a_B$

Material	Bandgap, eV	Exciton Bohr radius, nm
CdSe	1.84	4.9
CdS	2.58	2.8
ZnSe	2.82	3.8
CuCl	3.39	0.7
GaAs	1.52	12.5
Si	1.17	4.3

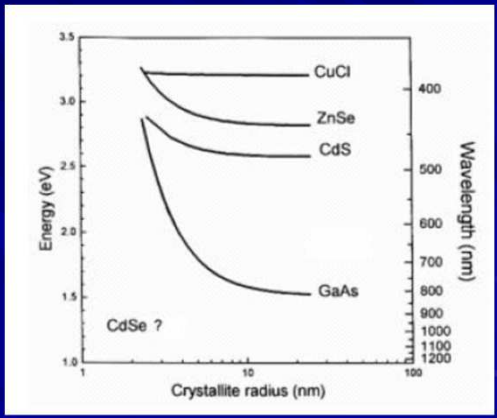

QD based solar cell

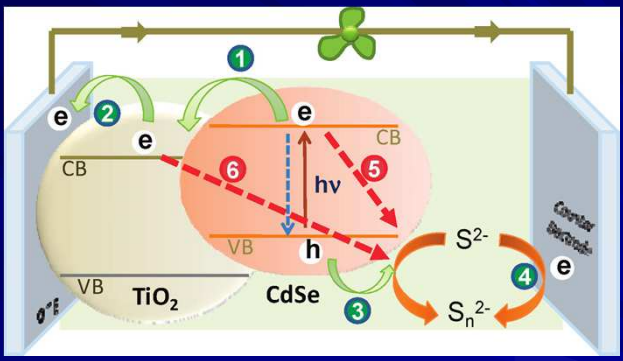

Redox electrolyte: I^-/I_3^-, polysulfide.
Counter electrode: Pt, Co, Cu_2S, etc..

Advantages of semiconductor quantum dots

- Quantum confinement allows for ***energy gap tunable*** across the solar spectrum.
- ***Large extinction coefficient*** resulting from quantum confinement.
- ***Large intrinsic dipole moment*** which may lead to rapid charge separation.
- Robust ***inorganic*** nature.
- Impact ionization occurs with the possibility of **high efficiency**.
- The ***predicted limiting efficiencies*** are 44.7% and 14-20% for QDSSCs and DSSCs, respectively.

Enhanced photovoltaic efficiency in QD solar cells by impact ionization (inverse Auger effect).

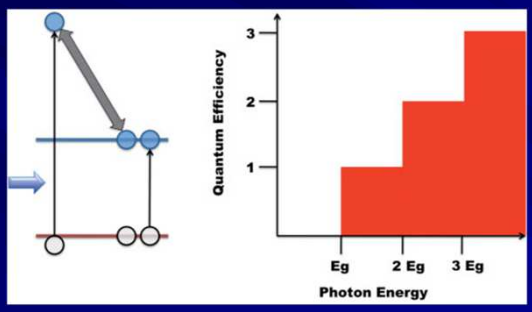

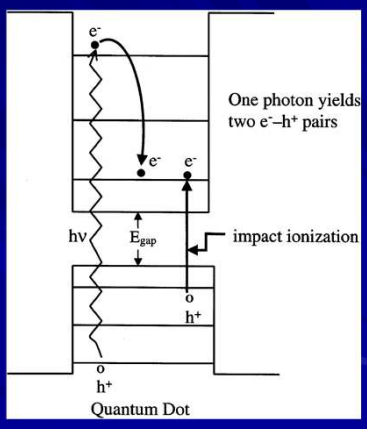

Multiple excitons generation (MEG)
QY=# e-h pairs/absorbed photons >1

QD based solar cell

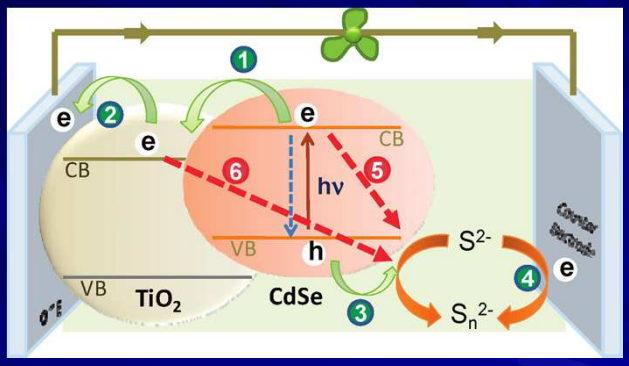

Redox electrolyte: I^-/I_3^-, polysulfide.
Counter electrode: Pt, Co, Cu_2S, etc..

QD solar cell

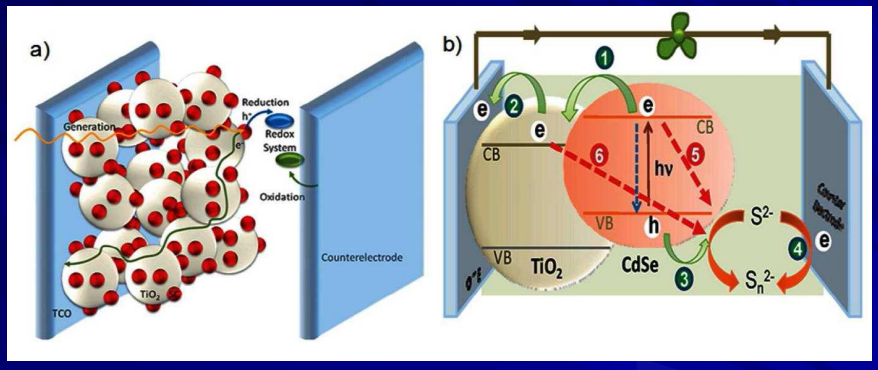

The predicted limiting efficiencies are 44.7% and 14-20% for QDSSCs and DSSCs, respectively.

Light-induced charge separation

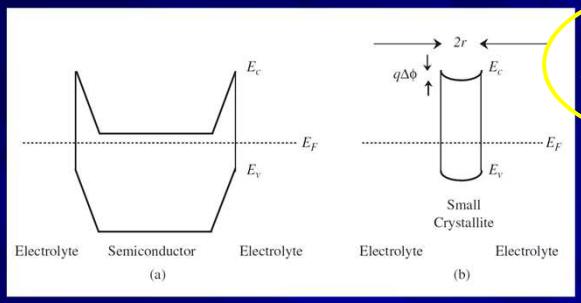

For a typical p-n junction, $\Delta\Phi$=728 mV

r=6 nm, N_D=5x10^{19} cm^{-3}, $\Delta\Phi$= 50 mV

$$\Delta\Phi = \frac{kT}{6q}\left(\frac{r}{L_d}\right)^2$$

Debye length:

$$L_d = \sqrt{\varepsilon kT / 2q^2 N_D}$$

SC-metal junction formation: work function

- Φ_m, work function.
- *X*, semiconductor electron affinity.
- Φ_S, work function.

Work function: *energy required to remove an electron from the highest filled level in the Fermi distribution of a solid to vacuum.*
Is a fundamental electronic property of any material which determines the band alignment in the contact at the heterojunction to facilitate selective electron and hole transport.

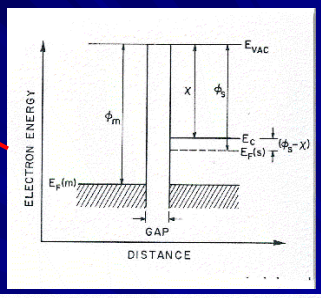

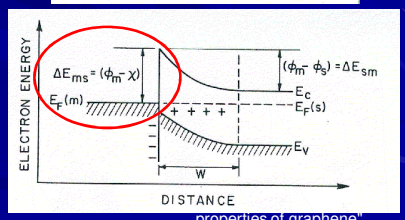

properties of graphene", Universitá di Roma "La Sapienza", November 13, 2017

Light-induced charge separation

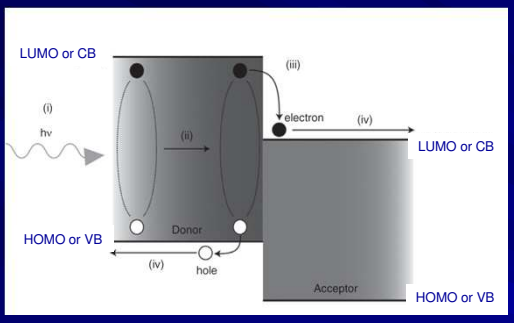

i) Absorption of a photon creates an exciton.

ii) Diffuses to an interface between the donor and the acceptor.

iii) Exciton dissociation at the donor-acceptor interface (free charge carriers).

iv) Free charge carriers transported out the device.

The ***band offset*** must be greater than the exciton binding energy for dissociation to occur.

$$\chi^A - \chi^D > U_{Exciton}$$

χ, electron affinity;
$U_{Exciton}$, the coulombic binding energy of the exciton on the donor .

Energy-level alignment with the metal-oxide electrode materials.

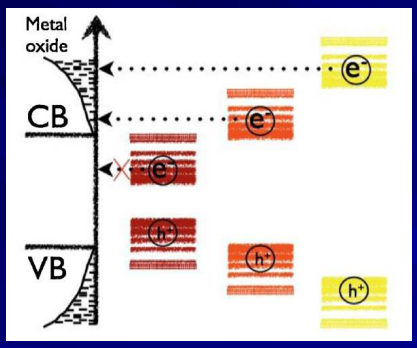

Tuning the bandgap energy value (the conduction band edge energy), then the charge injection.

MO Donating species

accepting species

Modelling electron transfer in QD-MO nanoparticulate systems

$$k_{ET} = \frac{2\pi}{\hbar}\int_{-\infty}^{\infty}\rho(E)|\bar{H}(E)|^2\frac{1}{\sqrt{4\pi\lambda k_B T}}e^{-\frac{(\lambda+\Delta G+E)^2}{4\lambda k_B T}}$$

Marcus model describing electron transfer from a single donating state to a continuum of accepting states, such as those present in the conduction band of a semiconductor.

Where: k_{ET} is the electron transfer rate, $\hbar$ is the reduced Planck's constant, k_B is Boltzmann's constant, λ is the system reorganizational energy, and *H(E), ρ(E),* and ***ΔG*** are the overlap matrix element, density of accepting states, and ***change in system free energy***.

ΔG free energy change associated with moving the electron from the donating species to the accepting species

$$\Delta G = E_{MO} - E_{1Se} + \frac{e^2}{2R_{QD}} + 2.2\frac{e^2}{\varepsilon_{QD}R_{QD}} - \frac{e^2}{4(R_{QD}+h)}\frac{\varepsilon_{MO}-1}{\varepsilon_{MO}+1},$$

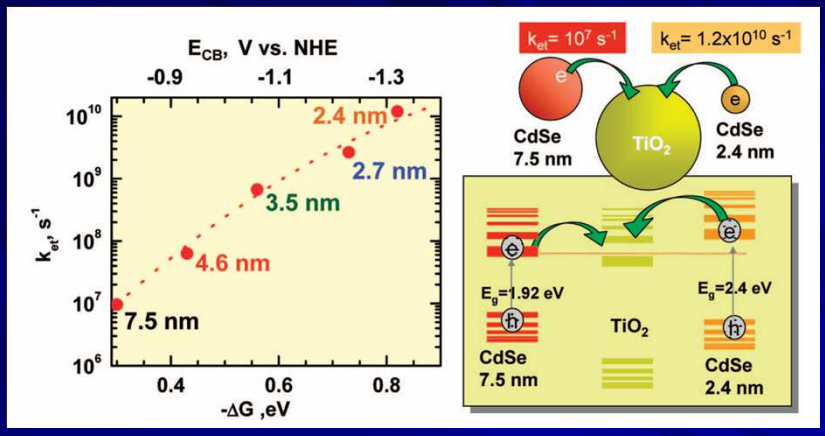

The driving force (-ΔG) for the electron transfer between CdSe and TiO_2 is dictated by the energy difference between the conduction band energies.

Solar cells by design

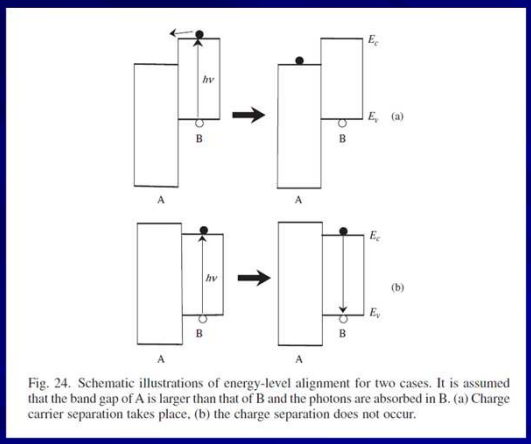

Fig. 24. Schematic illustrations of energy-level alignment for two cases. It is assumed that the band gap of A is larger than that of B and the photons are absorbed in B. (a) Charge carrier separation takes place, (b) the charge separation does not occur.

Therefore, the ability of light-induced charge separation is governed by the band position of materials.

Solar cells by design

Fermi level alignment

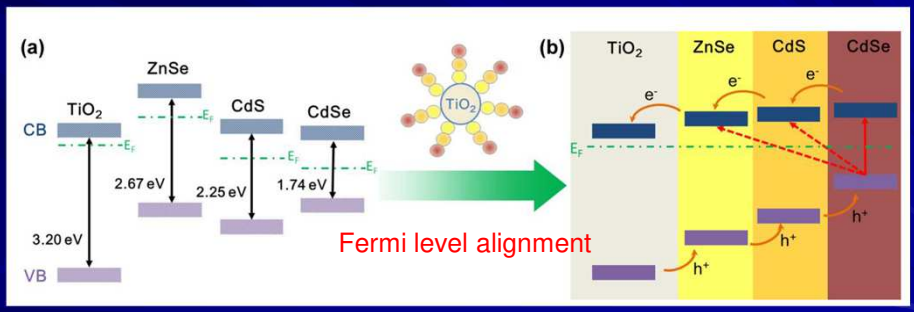

Lin Yang et al., Nanoscale, 7, 3173, 2015.-

Solar cells by design

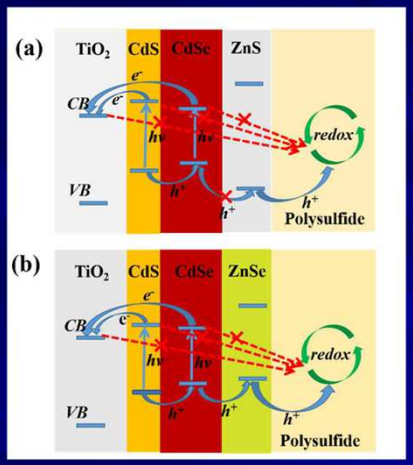

Passive layer and blocking layer.

η= 3.42, 4.91 and 6.39%

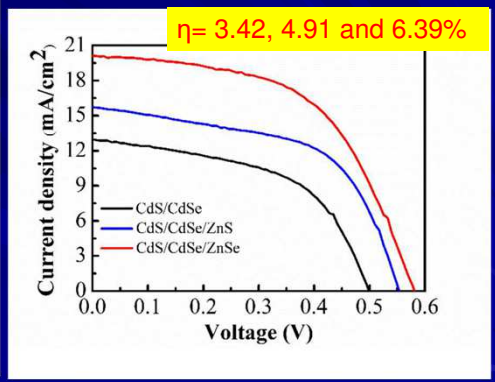

F. Huang et al., J. Mater. Chem. A, 4, 14773, 2016.-

Schematic diagrams of electron transfer processes

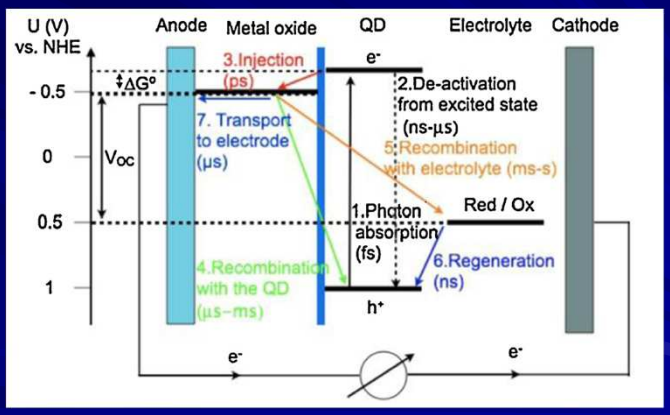

Materials used as electron transporting phase.

Ideally, a suitable electron acceptor for QDSSCs should fulfill the following conditions:

- Appropriate conduction band edge position for enabling electron injection.
- Moderate-high surface area to load enough QDs to harvest most of the irradiated photons.
- Open structure (wide and interconnected pores) allowing for a facile penetration/adsorption of colloidal QDs and filling with hole transporting phase.
- High electron mobility to efficiently collect photoinjected electrons.
- Poor light absorption in the visible region together with scattering effects to favor QD light-harvesting.
- Easy fabrication.

Materials used as electron transporting phase.

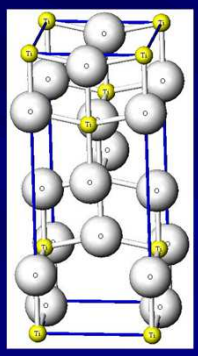

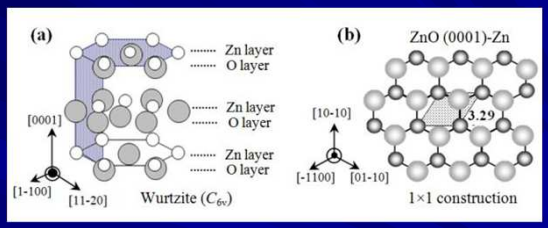

TiO_2 ZnO

ZnO vs. TiO_2

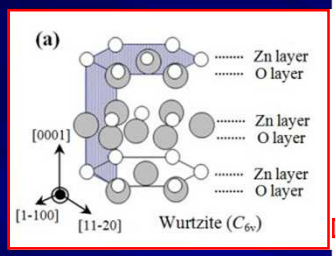

Table 1
Selected material properties of single-crystalline ZnO and TiO_2

		ZnO	TiO_2	Unit	References
Crystal structure		Wurtzite	Anatase		
Lattice constant, a		3.25	3.78	Å	[110, 111]
Lattice constant, c		5.12	9.51	Å	[110, 111]
Density		5.6	3.79	g cm^{-3}	[30, 110]
Static dielectric constant	ε_s	7.9	31		[112, 113]
Optical dielectric constant[a]	ε_∞	3.7	6.25		[30, 113]
Optical band gap	E_{opt}	3.2	3.2	eV	[22, 114]
Flat band potential[b]	E_{fb}	−0.5	−0.5	V vs. SCE	[20, 22]
Effective electron mass	M^*	0.24–0.3 m_e	1.0 m_e	$m_e = 9.11 \times 10^{-31}$ kg	[37, 114–116]
Effective hole mass	m_h^*	0.45–0.6 m_e	0.8 m_e	$m_e = 9.11 \times 10^{-31}$ kg	[37, 115, 116]
Electron mobility[c]	μ_e	200	30	cm^{2}V^{-1}s^{-1}	[117–119]
Point of zero charge	PZC	8–9	5.5–6.5	pH	[24, 25]

[a] ε_∞ for anatase was calculated from n^2 from Ref. [30].
[b] The value from Ref. [20] is recalculated to pH = 5 with a Nernstian shift of −59mV/pH.
[c] Hall mobility for the n-type materials at 300 K.

ZnO, estructura wurtzita,
tipo-n (vacancias O e intersticiales Zn),energía exciton: 60 meV, crece bajo diferentes morfologías, piezoelectricidad, etc..

TiO_2: effect of nanostructuring

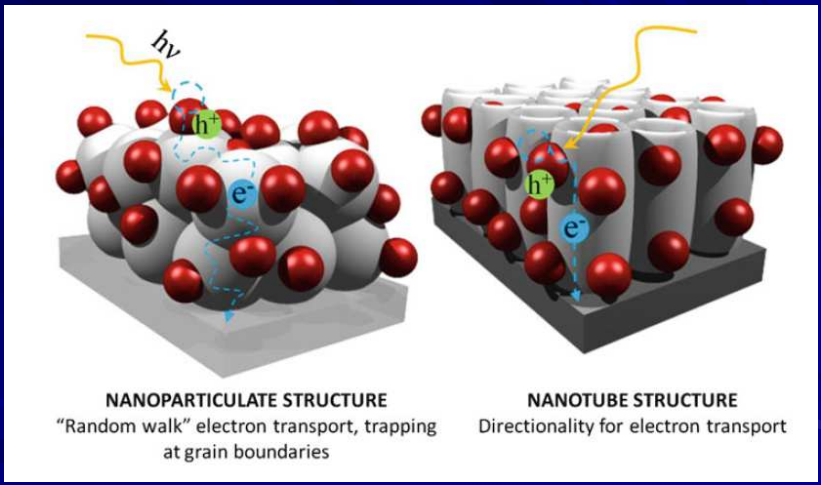

Comparison of electron mobilities for 1-D nanomaterials and nanoparticles.

Nanomaterials	Electron mobilities ($cm^2\ V^{-1}\ s^{-1}$)
SWCNT	7.9^a–$10^b \times 10^4$
Si nanowire	1000^c
Ge nanowire	600–700^d
ZnO nanowire	1–5^e
ZnO nanoparticle film	0.017–0.066^f
TiO_2 nanoparticle film	$<10^{-3g}$

[a] Field-effect and; [b] intrinsic mobility of a 300 nm long and 3.9 nm diameter single-walled carbon nanotube (SWCNT) [50]; [c] 8–30 nm wide Si nanowires [51]; [d] 20 nm wide Ge nanowires [52]; [e] 16–17 μm long and 130–200 nm wide ZnO nanowire [23]; [f] for particle size around 4 nm [53]; [g] for 4–8 nm anatase TiO_2 nanocrystals; it is 15 $cm^2\ V^{-1}\ s^{-1}$ in single crystal TiO_2 [54]

IPCE: incident photon-to-current conversion efficiency for monochromatic radiation

$$IPCE(\lambda) = \frac{\#\ photogenerated - electrons}{for - each - incident - photon}$$

$$IPCE(\lambda) = \frac{1240 \times J_{SC}(Acm^{-2})}{P_{in}(Wcm^{-2}) \times \lambda(nm)}$$

$$IPCE(\lambda) = LHE(\lambda) \times \phi_{inj}(\lambda) \times \phi_{coll}(\lambda)$$

$$LHE(\lambda) = 1 - 10^{\alpha(\lambda)d}$$

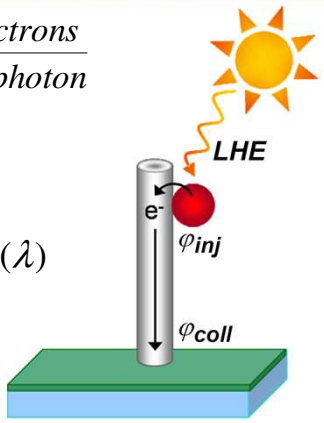

where ***LHE*** is the light-harvesting efficiency (the fraction of light that is absorbed at a specific wavelength), φ_{inj}, the quantum yield of charge injection and φ_{coll} the efficiency of collecting the injected charge at the back contact.

Quantum yield of charge carrier injection

- Competition with radiative or nonradiative recombination (deactivation channels).
- k_{inj}, injection rate.
- k_{deact}, sum of the rate constants of those nonproductive channels.
- Typical k_{deact} values 10^3 to 10^{10} s^{-1}, so injections rates in the ps range to obtain Φ_{inj} close to 1.

$$\phi_{inj} = \frac{k_{inj}}{k_{inj} + k_{deact}}$$

IPCE: incident photon-to-current conversion efficiency for monochromatic radiation

ZnO NWs/CdSe QDs

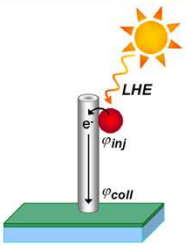

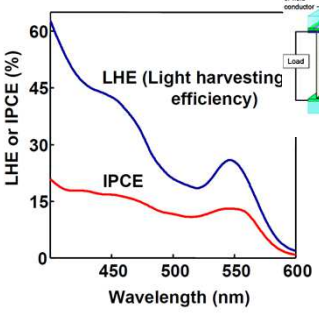

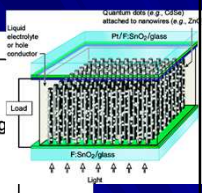

$$IPCE = LHE \times \underbrace{\varphi_{inj} \times \varphi_{coll}}_{IQE}$$

IQE=APCE

- Internal quantum efficiency (*IQE*) as high as 45–58% between 500–600 nm.
- Power conversion efficiency limited by the *LHE* and available nanowire surface area.

K.S. Leschkies et al., Nano Letters, 7, 1793, 2007.-

Photocurrent action spectra of CdSe QD-sensitized cells

TiO_2 NPs/CdSe QDs

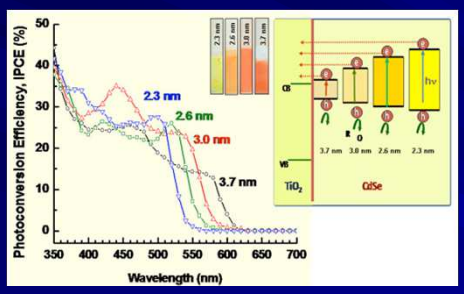

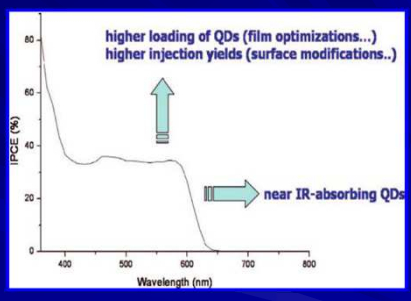

A. Kongkanand, J. Am. Chem. Soc. 2008, 130, 4007, H.J. Lee et al.,J. Phys. Chem. C 2008, 112, 11600.

How to improve the IPCE…

$$IPCE(\lambda) = LHE(\lambda) \times \phi_{inj}(\lambda) \times \phi_{coll}(\lambda)$$

- *LHE*: α↑, load QDs (thickness).
- Φ_{coll}:

$$L_n = \sqrt{D\tau}$$

A key parameter!

High-Efficiency "Green" Quantum Dot Solar Cells

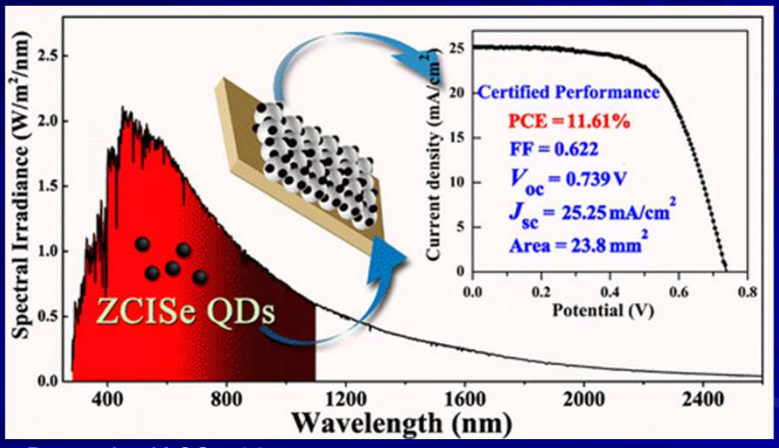

Jun Du et al., *JACS*, **138**, 4201-4209, 2016.

Timeline of energy conversion efficiency

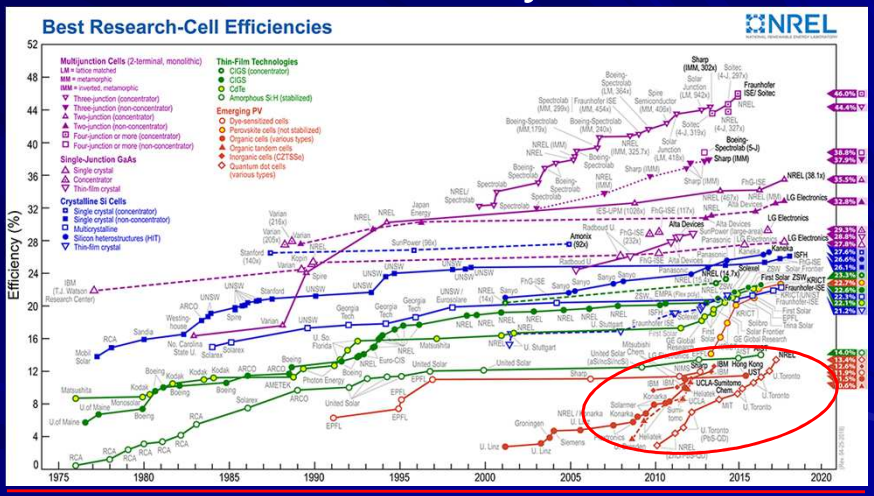

Solar cell generations

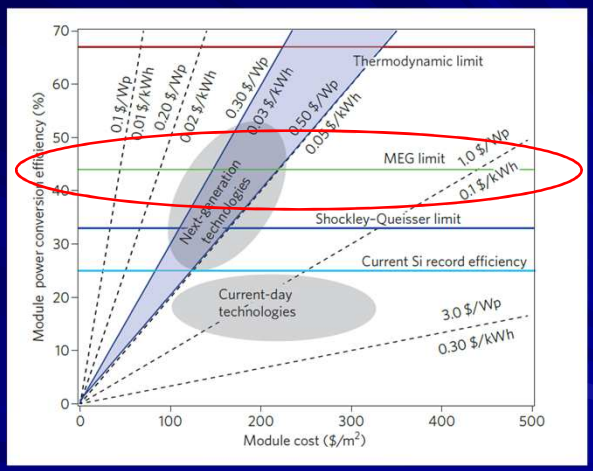

M.C. Beard, J.M. Luther, A.J. Nozik, *Nature Nanotechnology*, Vol. 9, 951, 2014.

Evolución celdas solares en base a QDs semiconductores

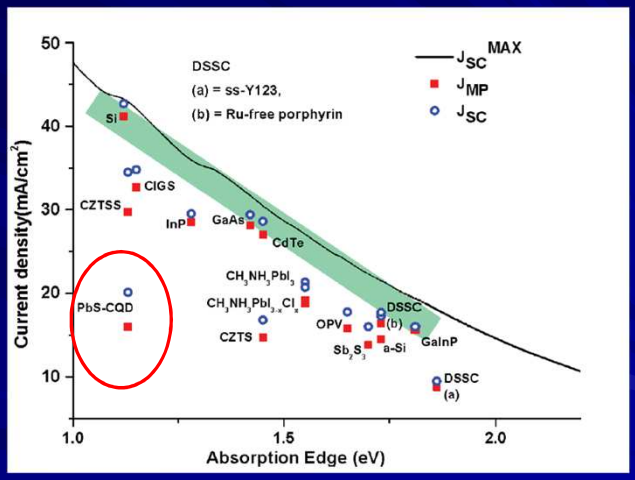

High-Efficiency "Green" Quantum Dot Solar Cells

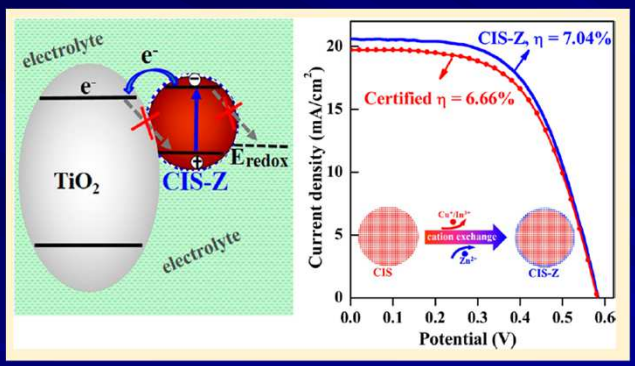

Surface passivation of the ternary $CuInS_2$ (CIS) QDs: provides high PV quality core/shell CIS/ZnS (CIS-Z) QDs.

J. Bisquert et al., J. Am. Chem. Soc. 2014, 136, 9203–9210.

SILAR asistido por rotación

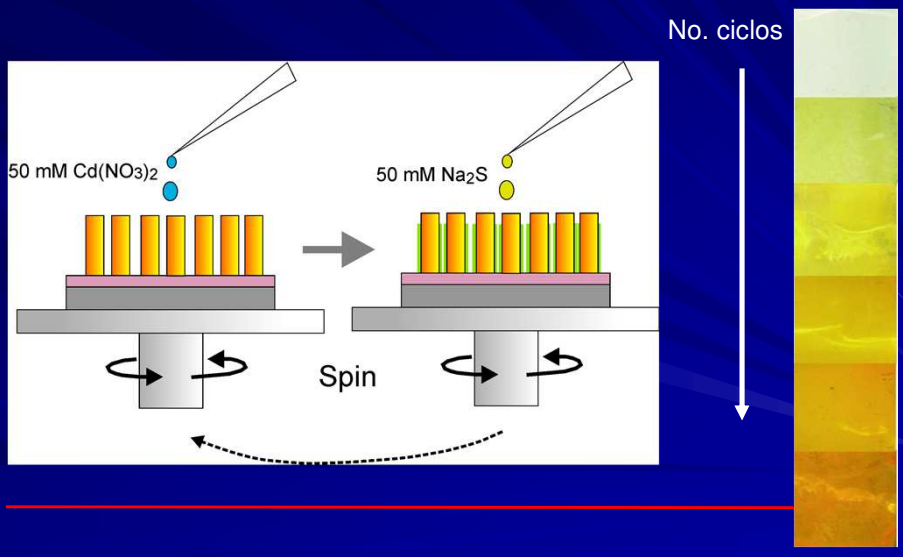

Tuning the ZnO nanowire diameters.

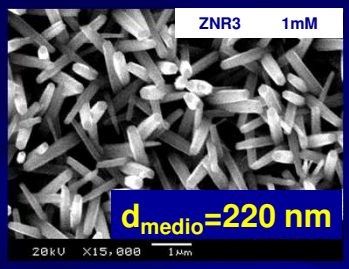

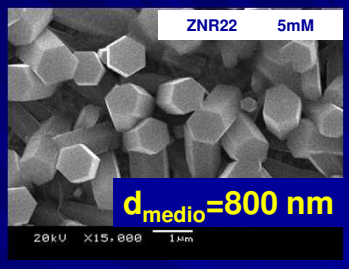

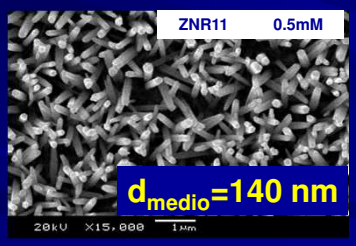

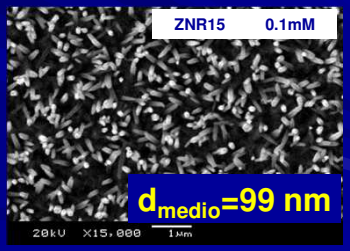

HRTEM of a single ZnO NR

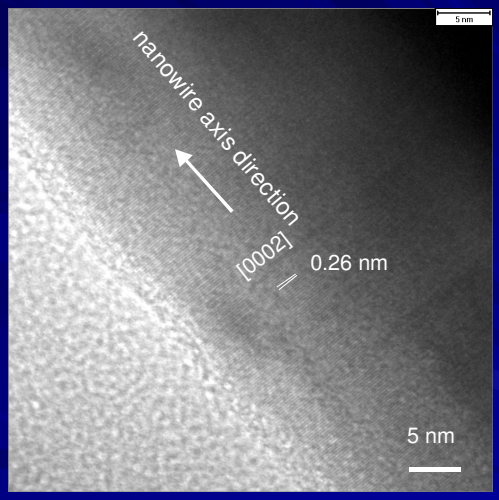

Caracterización TEM y HRTEM

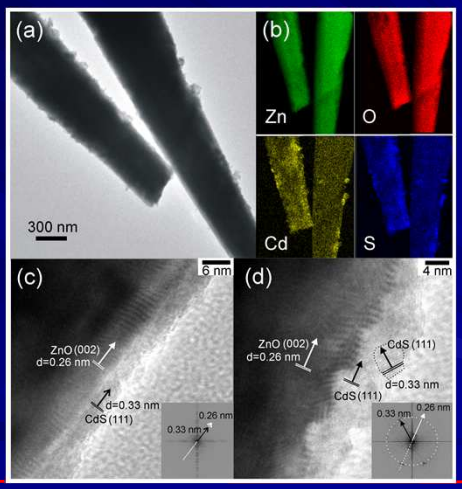

Caracterización XRD

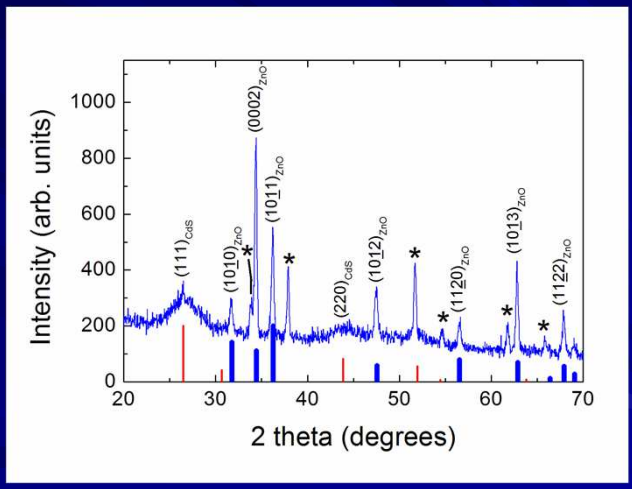

Propiedades ópticas

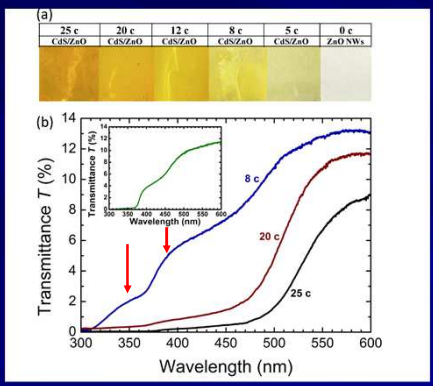

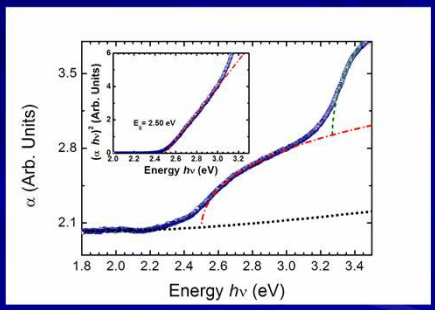

The absorption edges located at the UV are assigned to FTO substrate (between 300 and 350 nm), and ZnO NR (between 350 and 390 nm) .

Caracterización PEC

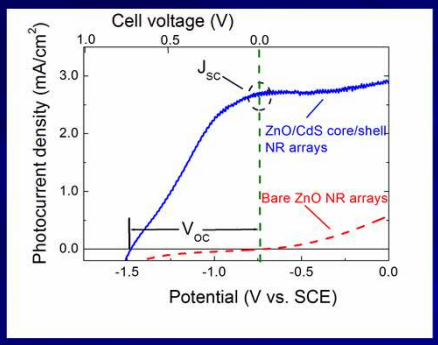

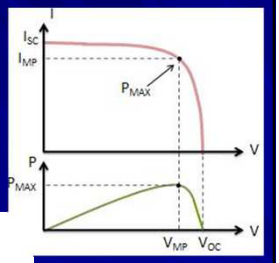

- Lámpara halógena.
- P_{in}=40 mW/cm^2
- η=1.48%

$$\eta = \frac{P_{out}}{P_{in}} = \frac{V_m I_m}{P_{in}}$$

$$FF = \frac{V_m I_m}{V_{OC} I_{SC}}$$

$$\eta = \frac{P_{out}}{P_{in}} = \frac{V_{OC} I_{SC} FF}{P_{in}}$$

Number of Publications

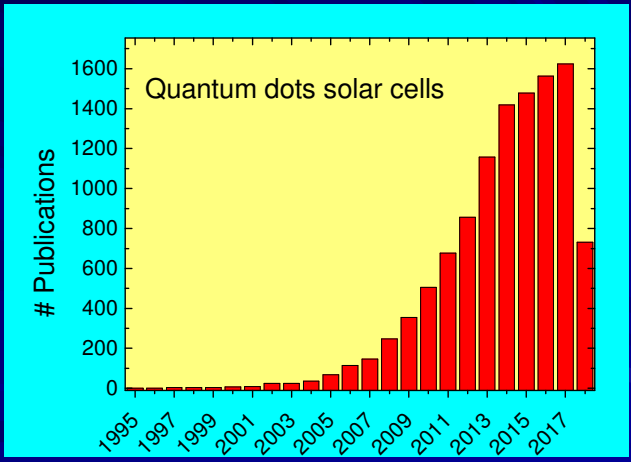

Challenges…

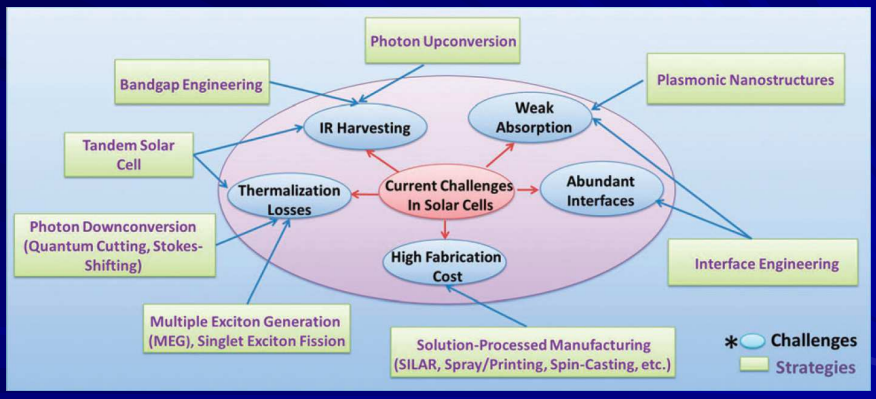

Efficiency improvement in QDSSC

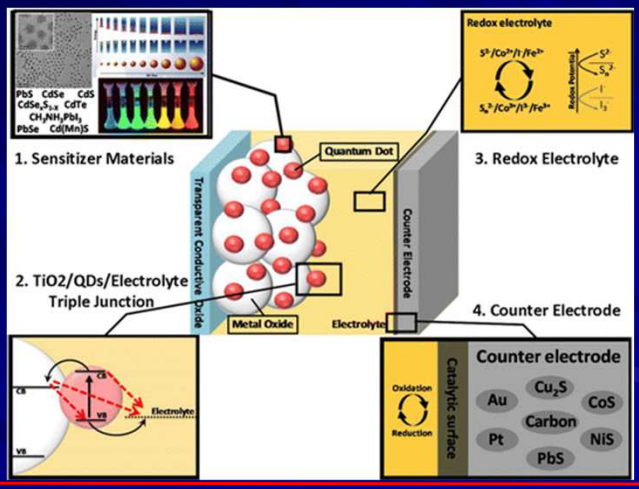

Efficiency improvement in QDSSC

The efficiency improvement in QDSSC may be attributed to both:

- materials development.
- the progress in understanding the cell mechanisms.

Materials development

- The emergence of absorbers such as PbS, PbSe, and Sb_2S_3, which extend the light absorption range from the visible to the near-infrared (NIR) region.
- The improvement of QD synthesis and loading using successive ionic layer adsorption and reaction (SILAR), chemical bath deposition and electrophoretic deposition (EPD).
- Different morphology of wide bandgap semiconductors.
- New counter electrodes.
- The improvement of the redox couple electrolyte.

Efficiency improvement in QDSSC

The efficiency improvement in QDSSC may be attributed to both:

- materials development.
- the progress in understanding the cell mechanisms.

Progress in understanding the cell mechanisms.

- The existence of several electron injection paths, directly from the conduction band of the QD and via surface states.
- Fast hole extraction relative to electron recombination with the electrolyte.
- Charge accumulation in the QDs layer that modifies the electronic properties of the QD layer upon illumination.
- The effect of surface modifications of both the QDs and the metal oxide that can reduce the recombination rates within the QDSSC.